# D4.2 Report on process and emission measurement technology for $H_2$-combustion systems

Andreas Koeppen, Carolin Lohrberg, Claudia Schrodt, Manav Matroja, Martin Oberlaender, Philip Lindner | Endress+Hauser SICK GmbH+Co.KG

Emilia Rontti | Luxmet Ltd

Arto Rautioaho, Henri Pauna | University of Oulu

June 2025

HYINHEAT

## Credits

## Disclaimer

This project has received funding from the European Union’s Horizon Europe research and innovation programme under grant agreement No 101091456.

## Technical references

| Grant Agreement N° | 101091456 | Acronym | HyInHeat |
|---|---|---|---|
| Full Title | Hydrogen Technologies for Decarbonization of Industrial Heating Processes | | |
| Work Package (WP) | WP4 – Instrumentation and algorithms for measurements and controls – Combustion control and Emissions monitoring | | |
| Authors | Andreas Koeppen, Carolin Lohrberg, Claudia Schrodt, Manav Matroja, Martin Oberlaender, Philip Lindner (Endress+Hauser SICK GmbH+Co.KG)<br>Emilia Rontti (Luxmet Ltd)<br>Arto Rautioaho, Henri Pauna (University of Oulu) | | |
| Leading organisation | Endress+Hauser SICK GmbH+Co.KG | | |
| Date of publication | 30.06.2025 | | |
| Contributors | Endress+Hauser SICK GmbH+Co.KG<br>Luxmet Ltd<br>University of Oulu | | |
| Document Type | R – Document, report | | |
| Document Title | Report on process and emission measurement technology for H2-combustion systems | | |
| Dissemination Level | PU – Public | | |

## Document history

| Version | Date | Partner | Author |
|---|---|---|---|
| 1 | 18/06/2025 | EHS | Andreas Koeppen |
| Final | 30/06/2025 | EHS | Andreas Koeppen |

## Contents

## Tables & Figures

## List of abbreviations

| Abbreviations | Explanation |
|---|---|
| DOAS | Differential optical absorption spectroscopy |
| EHS | Endress+Hauser SICK GmbH+Co.KG |
| EOS | Equation of state |
| HT | High temperature |
| ICAD | Intra cavity absorption detection |
| IFC | Interference filter correlation |
| IR | Infrared |
| OES | Optical emission spectroscopy |
| PEMS | Predictive emission monitoring system |
| SOS | Speed of sound |
| TRL | Technical readiness level |
| USM | Ultrasonic measurement |
| UV | Ultraviolet |
| VIS | Visible |
| WP | Work package |

# 1. Introduction

The actions in work package 4 (WP4) of the HyInHeat project to address fuel gas characteristics and flows involve the cross-sectorial utilization of two measurement technologies for fuel quality determination and the implementation of these into a lab-scale test rig and two demonstrators. One combines flow and fuel quality measurement in one calibrated measurement device providing a cost competitive option.

Furthermore, combustion control and $NO_x$ emission measurement technologies for $H_2$/air and $H_2/O_2$ fired processes are developed. To promote digitalization of production processes, data analysis and development of data-based digital process control algorithms will be performed in WP4. These solutions will be implemented in the demonstrators in WP5 and WP6 with the goal to provide interdisciplinary guidelines for process control and $NO_x$ emission measurement in WP7 and standardization in WP8.

# 2. Overview work package 4

WP4 “Instrumentation and algorithms for measurement and control” started in month 4 of the project and continued until month 30. The WP4 consists of five tasks and is coordinated by the work package leader Endress+Hauser SICK GmbH+Co.KG (EHS).

Initially, the work package was planned to end after month 24. But due to the set-up of the joint venture of SICK and Endress+Hauser and further delays in the build-up of the extractive spectroscopic analyser the deliverables were postponed by six months.

In this work package the sensors and analysers were improved and developed to provide instrumentation and algorithms needed for optimization of the $H_2$ combustion processes and emission measurement in the demonstrators at C-TEC and SWERIM. One is a reverberatory furnace at C-TEC for aluminium recycling (corresponds to task 5.3). At SWERIM, there is a walking beam furnace for heating steel slabs (corresponds to task 6.2). All five subtasks of WP4 are assigned to the corresponding process points which are seen in Figure 1.

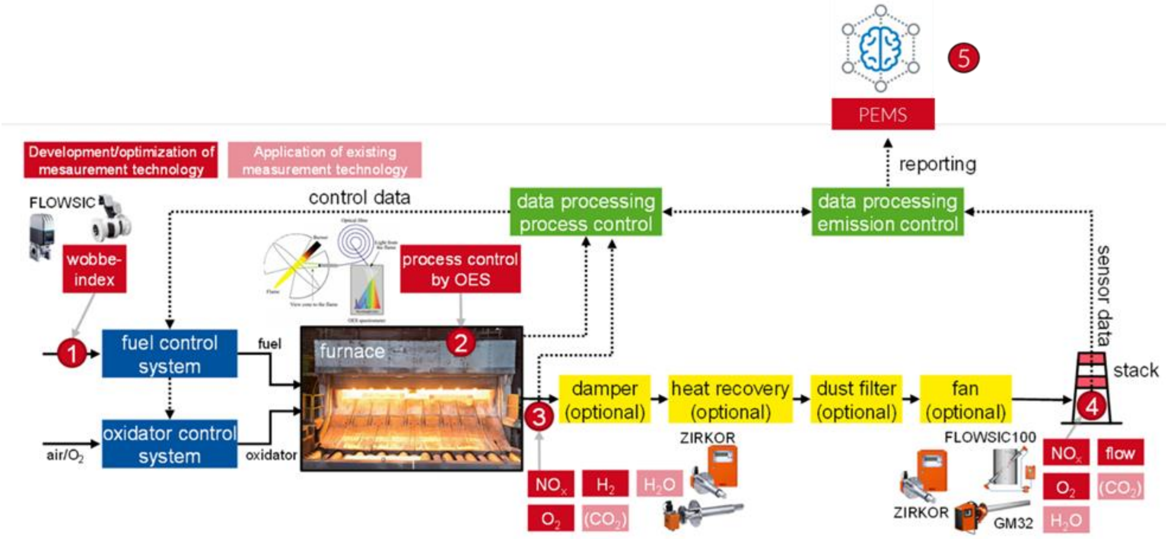

*Figure 1: Measurement points from MP1 to MP5 related to the tasks*

Due to the different furnace installations at C-TEC and SWERIM, different sensors and analysers were identified to be used. The following Table 1 gives an overview of the planned sensors and analysers and at which measuring points they will be installed. This is result of on-site visits of SICK at C-TEC and SWERIM. In general, it is intended that all the equipment is ready for installation on site by end of 2024, which fits to the overall project planning.

*Table 1: Overview of sensors/analysers for installation at C-TEC and SWERIM*

| Measuring Point | Sensors / Analysers | Measured variables | C-TEC | SWERIM |
|---|---|---|---|---|
| MP1 | H2 USM | Flow, Wobbe index | -- | -- |
| MP1 | Extractive spectroscopic analyser | Wobbe index | X | -- |
| MP2 | OES | Flame temperature<br>$H_2O$, Na, K | X | X |
| MP3 | Lamtec sensor I | COe, $O_2$ | X | X |
| MP3 | Lamtec sensor II | NOx, $O_2$ | X | X |
| MP3 | MCS300P (IR analyser) | CO, $CO_2$, $CH_4$, NO, $NO_2$, $H_2O$, $O_2$ | X | -- |
| MP3 | UV DOAS analyser | NO, $NO_2$ | X | -- |
| MP3 | GM35 | CO, $CO_2$, $H_2O$ | -- | X |
| MP4 | HT USM | Flow, temperature | -- | X |
| MP4 | GM32 | NO, $NO_2$ | -- | X |
| MP4 | ZIRKOR | $O_2$ | -- | X |
| MP5 | PEMS | Calculation of gas concentrations | X | X |

The main objective for this work package is to provide the instrumentation and algorithms needed for optimization of the $H_2$ combustion processes by on-line process control as well as on-line NOx monitoring for emission reduction and reporting. WP4 therefore provides the tools needed for the optimization of processes and emission measurement in WP5/6 and a valuable basis for the evaluation of NOx limits in WP7 and standardization in WP8.

## 3. Task 4.1: Wobbe index measurement technology

*$H_2$ ultrasonic measurement device*

For estimating the quality of the supplied hydrogen an ultrasonic flow meter with newly developed algorithms is used. The algorithms are based on the measurement of the speed of sound (SOS) and the gas temperature and estimates the purity of the hydrogen in binary mixtures with a known pollutant (i.e., nitrogen).

$H_2$ has a much higher speed of sound than all relevant gases that can appear as impurities in most applications. Adding only small amounts of these gases to pure hydrogen leads to a significant reduction of the speed of sound of the mixture. It is therefore possible to detect and estimate very low quantities of impurities by using algorithms that compare the SOS measured by the ultrasonic measurement (USM) flow meter to the expected SOS of pure hydrogen. Two such algorithms have been developed and tested by EHS as part of work package 4. One uses easy to compute pre-trained models, which makes it suitable for devices with a focus on low power consumption and also for older devices with low computing power. The other uses a suitable equation of state (EOS) for gas mixtures, e.g. GERG-2008, integrated into the device firmware. This makes the algorithm harder to compute but enables more possibilities in terms of process conditions and gas species.

Both algorithms use the SOS measured by the USM, as well as measurements of temperature and pressure of integrated sensors, and estimate the molar fractions of hydrogen and the known impurity gas. Additional properties like heating value or Wobbe index can then be calculated using established methods like ISO 6976.

The $H_2$ ultrasonic flow meter was part of WP3.5. Due to line size constraints the flow meter was not included in the RWTH-IOB's burner laboratory and cannot be installed at SWERIM or C-TEC. Instead, simulations and experimental verification measurements were done at EHS to evaluate the performance of the device and algorithms. All the measurement results were already published in the D3.4 report.

*Extractive spectroscopic analyser*

A spectroscopic analysing system was identified as an appropriate measurement device to accurately measure the Wobbe index of mixtures between hydrogen and natural gas. The system was built up, tested in the laboratory and will be shipped to C-TEC. It measures the full spectrum and is not based on gas chromatography technology. Based on that the concentrations of the gas components and further the calorific value and Wobbe index are calculated by using an own developed model. This product is currently still under development but has already undergone field trials in harsh process surroundings. Specific adaptations of the analysing system itself were not required. However, the extractive sampling system had to be adapted to the specific process conditions at C-TEC. All other connection points to the local infrastructure also had to be adapted.

Before shipping, the spectroscopic analyser was tested in the laboratory. A typical natural gas mixture with known concentrations (including uncertainties) was applied to the analyser straight from the bottles. Nominal values were calculated following the calculation procedure specified in ISO 6976, including uncertainties propagating from the concentrations. The measurement values from the spectroscopic analyser were compared to these nominal values. For the Wobbe index values, the relative deviation between measurement values and nominal values were smaller than the uncertainty on the nominal value. Therefore, the test was regarded as successful.

Table 2: Comparison of measurement values from the spectroscopic analyser with nominal values.

| Gas property | Measurement value | Nominal value | Relative deviation |
|---:|---|---|---|
| Wobbe index (gross) | 53.835 $MJ/m^3$ | 53.815 $MJ/m^3$ (± 0.11 %) | 0.04 % |
| Wobbe index (net) | 48.705 $MJ/m^3$ | 48.682 $MJ/m^3$ (± 0.12 %) | 0.05 % |
| Calorific value (gross) | 43.564 $MJ/m^3$ | 43.446 $MJ/m^3$ (± 0.26 %) | 0.27 % |
| Calorific value (net) | 39.412 $MJ/m^3$ | 39.302 $MJ/m^3$ (± 0.27 %) | 0.28 % |

The system was complemented by an analyser from the third-party supplier MEMS AG. This analyser is commercially available, has shown compliance with the OIML R140 requirements and uses a correlative measurement approach. Therefore, a comparison between the spectroscopic and the correlative technology will be possible based on the measurements during the operation at C-TEC. Since the MEMS AG analyser is not directly compatible with the specific process conditions at C-TEC, the extractive sampling system was adapted such that the MEMS AG analyser could be integrated.

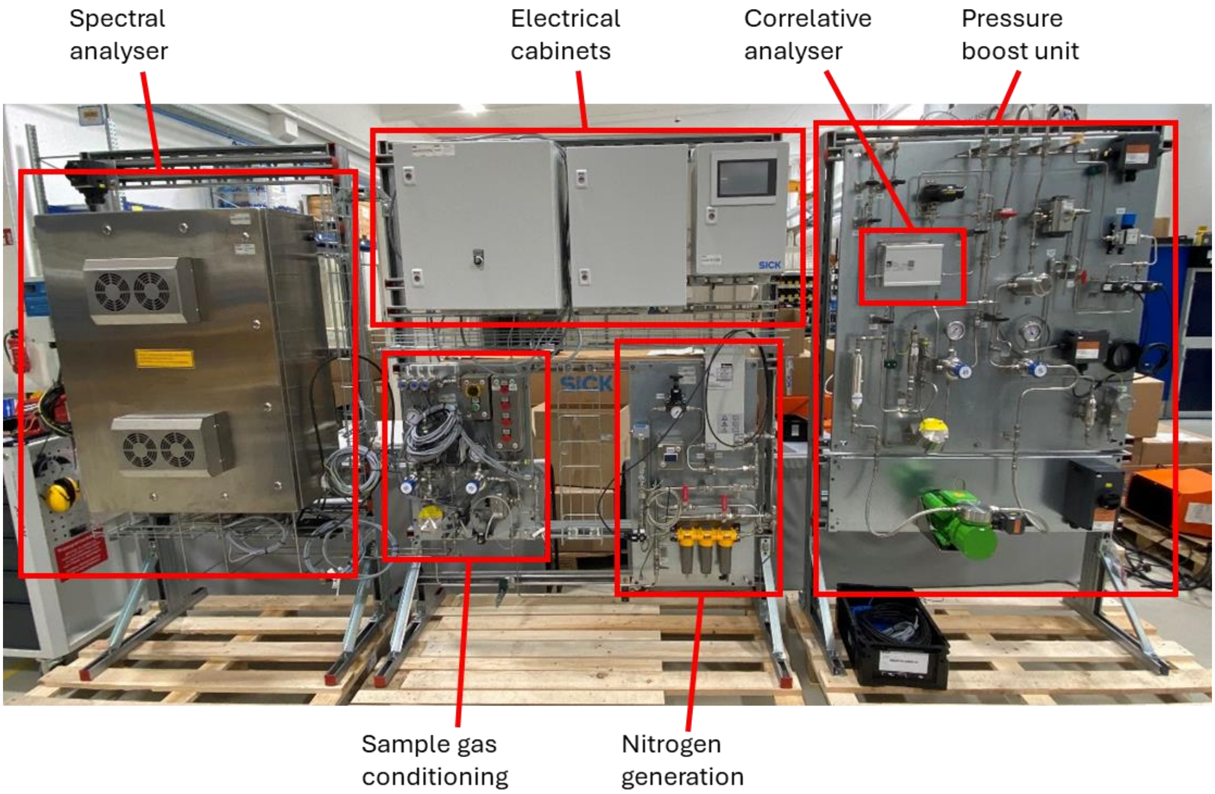

*Figure 2: Extractive spectroscopic analysing system, which measures the Wobbe index. The system will be installed at C-TEC.*

# 4. Task 4.2: OES measurement technology and combustion control

Optical emission spectroscopy (OES) has been proven to be a valuable method for analysing electric furnace processes. For example, it can be used to monitor the time development of chemical compounds and temperature. This information can be used to monitor the state of the process. This project aims to extend the usability of OES to burner-related processes. A similar technique has been used for a long time in fundamental research in physics and chemistry, but it has not been previously studied from the perspective of industrial flame analysis. The aim of this project is to generate knowledge about the applicability of the OES method for flame analytics, and the research questions can be summarized as follows:

1. Which parameters OES can provide from the flames and furnaces?
2. Are there some limitations to the usability of OES in furnaces?

Fundamental research has demonstrated that the OES method can be used to measure chemical compounds from flames and determine temperature under laboratory conditions. However, industrial environments introduce several practical challenges to conducting such measurements. This project aims to identify solutions to the practical challenges that industrial environments present for OES-based flame analysis and assess whether the method can still be effectively used for flame analytics.

## 4.1. Background of optical emission spectroscopy

The origins of optical spectroscopy can be traced back to the 17th century, when it was discovered that light can be dispersed into its component colors using a prism [1]. During the 19th century, the connection between spectral lines and chemical elements became evident, and the study of spectra became more systematic. At that time, significant gaps existed in the understanding of elemental composition, and optical spectroscopy played a crucial role in advancing both chemistry and physics.

It quickly became clear that this method could be applied to any light source, making astronomy a natural area for optical spectroscopy research [2]. In the early days, photographic plates were used to capture spectra, resulting in long delays between data collection and analysis. While this was not a major limitation for fundamental research in chemistry, physics, or even astronomy, it effectively excluded the real-time monitoring of industrial processes.

Only much later, around the turn of the millennium, did advances in digital light detectors and the increasing computational power of computers make near real-time spectrum analysis possible. This breakthrough opened the door for a new range of industrial applications for optical spectroscopy.

Until now, research has primarily focused on the analysis of electric furnaces [3, 4, 5], but the goal of this project is to expand this scope to include industrial flame analysis.

## 4.2. Overview of laboratory experiments

Experimental work related to this project consists of tests in the laboratory of RWTH Aachen with an open flame burner and burner-heated furnace. Experiments in Aachen consist of two campaigns, the first in June 2023 and the second in April 2024. The first campaign aimed to create an overall picture of the usability of OES as a burner monitor method and focused on answering the following questions: what is possible to measure from the flames with OES, and are there some practical issues or problems? The second campaign focused on solving problems that were identified in the first campaign and further developing the measurement method.

### 4.2.1. Detailed description of the experiments

The objective of the 2023 experiments was to generate foundational knowledge on flame measurements and to identify potential practical challenges in applying optical emission spectroscopy to such measurements. The measurement campaign can be divided into two parts: open flame measurements and furnace measurements.

The goal of the open flame measurements was to evaluate the feasibility of flame diagnostics using the selected equipment under conditions free from external disturbances. Additionally, these tests aimed to compare hydrogen and natural gas flames, as well as to investigate the effects of different hydrogen-to-natural gas ratios. During the tests, the hydrogen-to-natural gas ratio was gradually adjusted, starting with 100 % natural gas and progressing in steps to 100 % hydrogen. The burner power and lambda value were kept constant throughout the measurements, but the hydrogen fraction was increased in 5 % increments, relative to the total power. The spectrometer continuously monitored the flame properties, providing a comprehensive overview of the impact of hydrogen on the natural gas flame at various mixing ratios, as well as foundational data on the flame spectra. This approach was used for both the open flame burner and furnace measurements.

The objective of the furnace measurements was to assess how the furnace environment influences the measurement process and to identify the key differences between open flame and furnace measurements.

The most critical observation from the 2023 measurements, in terms of the method's viability, was that radiation from the furnace wall presents significant challenges for analysis, particularly at longer wavelengths within the measurement range (roughly above 600 nm). This issue was considered in the 2024 measurements, which primarily focused on furnace conditions, although some additional open flame measurements were also conducted for validation.

The primary topic for the 2024 campaign remained the radiation emitted by the hot furnace walls and its impact on measurement accuracy. The fundamental measurement approach was the same as before, focusing on the spectral effects of different hydrogen and natural gas mixtures. However, the precise impact of different mixture ratios was less critical in these tests, leading to a coarser adjustment in gas ratios, with 10 % steps.

The most significant improvement in this series of measurements was the use of different spectrometers capable of detecting radiation down to the ultraviolet (UV) range, providing a more comprehensive understanding of the spectral characteristics under these challenging conditions.

## 4.3. Results of OES experiments

Below, the results of the executed experiments are listed. On the one hand open flame experiments were carried out, on the other hand furnace experiments were realized.

### 4.3.1. Open flame experiment

The open flame experiments were initially intended to serve only as reference measurements for the furnace tests, but they also yielded valuable research data. The most significant finding was the effect of hydrogen on flame radiative heat transfer at different shares of hydrogen. These results have been reported in open-access article [6], prepared as a part of HyInHeat project.

Radiation formation in flames can be broadly divided into two components: molecular emissions and grey body radiation, the latter resulting from soot (solid particulate) present in the flame. Molecular emissions produce relatively narrow-band radiation, leading to comparatively low radiative heat transfer. In contrast, solid surfaces like soot emit broadband grey body radiation, which means significantly higher radiative power. Given that soot originates from the carbon content of the fuel, it is intuitively clear that pure hydrogen flames, which contain no carbon, do not produce soot and therefore exhibit relatively low radiative heat output.

Many previous studies suggest that adding hydrogen to natural gas reduces soot formation and thermal radiation in a monotonic fashion. However, the experiments conducted as part of this project clearly demonstrated that small hydrogen fractions (5-19 %) actually increased soot production and, consequently, flame radiation (Figure 3) [6]. The exact mechanism behind this phenomenon could not be fully resolved within the scope of this study, but a possible explanation might involve the combined effect of the turbulent nature of the flame and the higher burning velocity of hydrogen relative to natural gas. This combination could lead to the formation of localized fuel-rich (sub-stoichiometric) regions within the flame, which are known to promote soot formation.

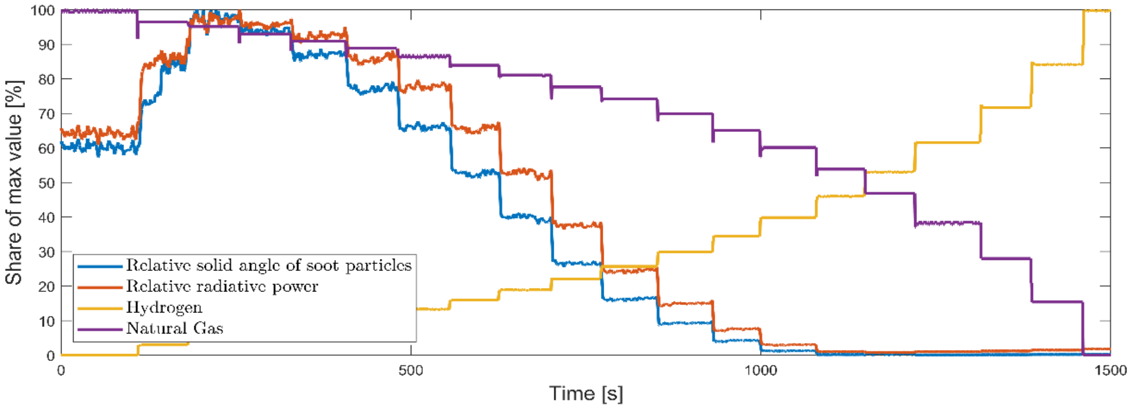

*Figure 3: The relative solid angle of soot particles corresponds to the radiating surface area of the soot within the measurement region. It can be observed that the amount of soot reaches its maximum when the share of hydrogen is approximately 5 %.*

Temperature measurements were also attempted from the open flame (Figure 4). This approach relies on the radiation emitted by soot particles, which approximately follows Planck's radiation law. This method enabled temperature determination for flames containing a measurable amount of soot. To improve the accuracy of the results, literature-based emissivity functions were used to estimate the spectral intensity of the soot radiation [7].

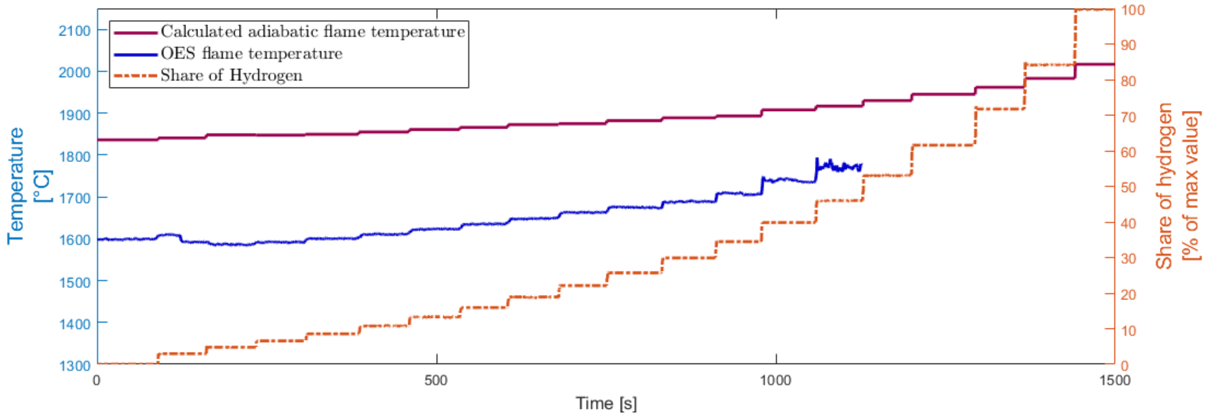

*Figure 4: Open flame OES temperature measurements. The calculated adiabatic flame temperature represents the theoretical maximum temperature of the flame. It can be observed that the difference between the measured and theoretical temperatures is inversely proportional to the radiative power of the flame (Figure 3).*

The measurements were successful up to a hydrogen fraction of approximately 46 %, beyond which the soot concentration became too low to provide a sufficiently strong signal for temperature determination. Another significant limitation was the lack of reliable reference data, preventing the accurate determination of absolute temperatures.

However, the observed temperature trends measured by OES exhibited a consistent and logical relationship with the theoretically predicted maximum flame temperatures as the fuel mixture was varied. This suggests that, despite the limitations, the OES method likely provides at least a qualitatively correct relative temperature change under these conditions.

### 4.3.2. Furnace experiments

The goal of the furnace experiments was to determine what type of information OES can provide about the furnace environment and to identify the challenges that such environments pose for OES measurements.

The primary challenge in these measurements is that the hot furnace walls emit intense thermal radiation, meaning that the measured signal is a combination of both the flame radiation and the wall radiation. This creates significant challenges for accurate measurements but does not necessarily prevent effective OES diagnostics in furnaces.

The radiance $L(\lambda,T)$ emitted by the furnace walls can be described by the temperature-dependent Planck radiation law $B(\lambda,T)$ and the material-dependent emissivity function $\varepsilon(\lambda,T)$ of the furnace wall:

$$L(\lambda,T) = \varepsilon(\lambda,T)B(\lambda,T)$$

According to Planck's radiation law, the peak intensity of the radiation emitted by the furnace walls falls within the infrared region, while the radiation in the ultraviolet (UV) range is essentially negligible. As a result, it was observed in the experiments that furnace wall radiation does not interfere with measurements in the UV range or at the shorter wavelengths of the visible spectrum. However, at the red end of the visible spectrum, the wall radiation becomes sufficiently intense to significantly disrupt the measurements. A rough cutoff for reliable measurements can be considered to be around 600 nanometers.

Consequently, monitoring the time development of molecular emissions with wavelengths below 600 nm was possible without significant interference (Figure 5).

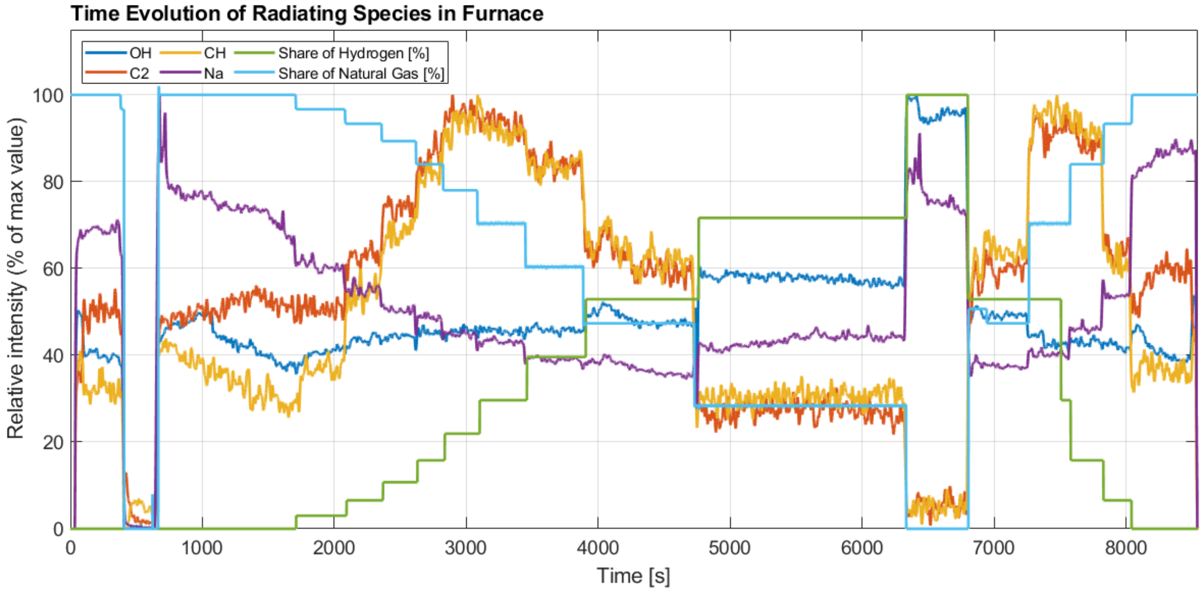

*Figure 5: Time evolution of OH, $C_2$, CH and Na measured by OES from the furnace.*

### 4.3.3. Removal of furnace background radiation from the spectrum

In the data analysis of furnace measurements, efforts have also been made to develop a technique for removing furnace background radiation from the measured spectrum. The principle for this approach is based on the previously discussed equation, which allows the prediction of wall radiation if the wall temperature and emissivity function are known.

The emissivity function can be determined by measuring the furnace wall spectrum when the burner is turned off, in which case the spectrum represents only the wall radiation at a given temperature. This wall spectrum can then be used, together with temperature data, to subtract the calculated spectral wall radiation from the measured spectrum. In principle, this should yield the pure flame spectrum.

At the time of writing, this method is still under development, but preliminary results suggest that it is highly promising and may significantly extend the previously reported 600 nm wavelength cutoff for accurate measurements. The main challenge for implementing this method is obtaining precise and real-time wall temperature data and integrating it effectively with the spectral measurements.

## 4.4. Optical emission spectroscopic measurement equipment for demonstrators

The OES measurement system is designed to analyse industrial burner flames at two locations: a walking beam furnace at SWERIM and a reverberatory furnace at C-TEC. Each site has its own dedicated set of equipment. This system is tailored for precise and reliable optical flame analysis in industrial processes.

### 4.4.1. Measurement head

The OES system collects light from burner flames using a robust measurement head, built to withstand high temperatures. It includes a continuous nitrogen flow for cooling and cleaning. The measurement head is installed inside a protective guide tube, which shields it from heat and splashes. A picture of an installed measurement head and guide tube is shown in Figure 6.

Figure 6: Installed OES measurement head and guide tube.

### 4.4.2. Measurement cable

The captured light is transmitted via a measurement cable to the equipment cabinet. The cable is optimized for ultraviolet light detection and is protected with thermal insulation. It is cooled with a continuous nitrogen flow. The cable length was defined based on installation requirements.

### 4.4.3. Equipment cabinet

The stainless-steel equipment cabinet houses electrical and pneumatic components. It enables real-time data collection and analysis and is designed for demanding industrial environments. The cabinet powers an industrial PC and spectrometer, while the pneumatic system provides cooling and maintains a clear optical view. A picture of an installed equipment cabinet is shown in Figure 7.

Figure 7: Installed OES equipment cabinet.

# 5. Experimental setup for combustion control and emission monitoring analysers (task 4.3 and task 4.4)

The biggest challenge for the analysers is the very high water content produced during the combustion of $H_2/O_2$ oxyfuel. For the analysers to measure efficiently, condensation must be avoided inside the analysers, as it can adversely affect the measured values. Further, water vapour can have a cross-sensitivity to other measuring components, which leads to incorrect measuring values. To address this, all the measuring solutions were tested in the laboratory under conditions simulating those expected in the project. High water vapour content is generated using a special vaporizer and it is mixed with different test gases such as NO, $H_2$, and $O_2$ etc. with the help of a gas mixer. The complete system is heated and maintained at 180 °C to prevent any condensation. It is shown in Figure 8.

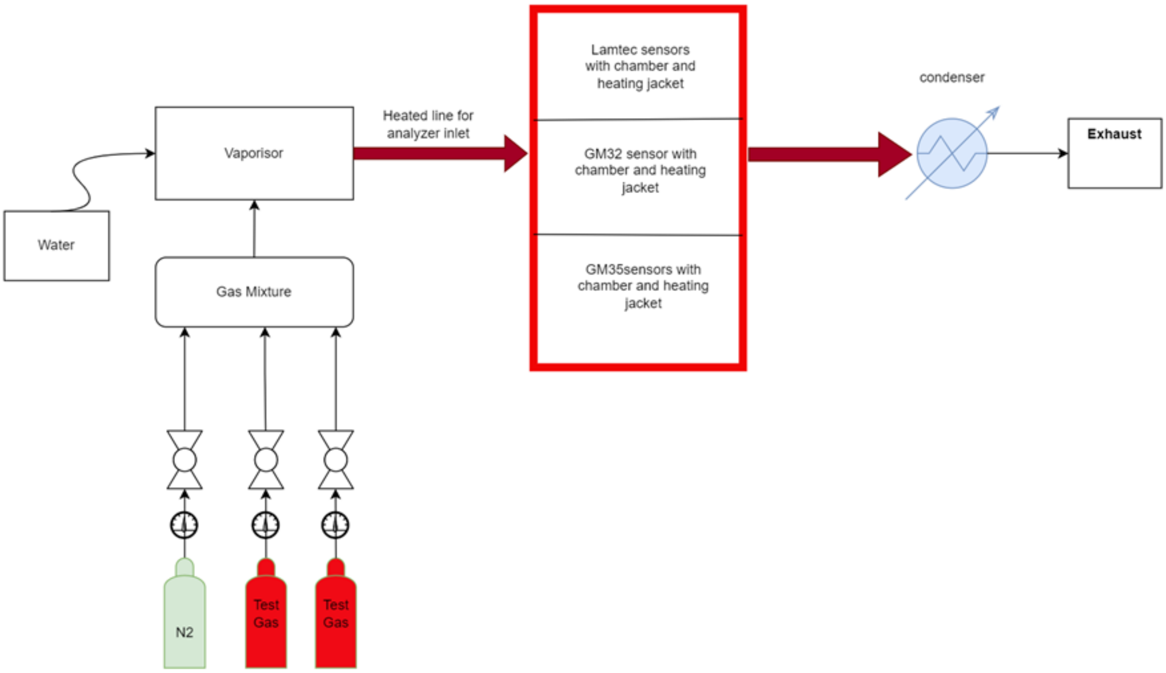

*Figure 8: Laboratory experimental setup*

Using a vaporizer, steam levels ranging from 0 % to nearly 95 % were generated. Since the GM35 analyser can measure up to 100 vol% of water vapours, the steam generation capability of the vaporizer was initially tested. It was possible to reliably generate and measure up to 80 vol% of steam using the GM35 with a relative error of approximately 2.5 % as shown in the figure below. However, beyond 80 vol%, the steam generation became inconsistent as shown in Figure 9 from the vaporizer affecting measurement reliability. Therefore, 80 vol% was set as benchmark for testing all analysers under consistent steam conditions.

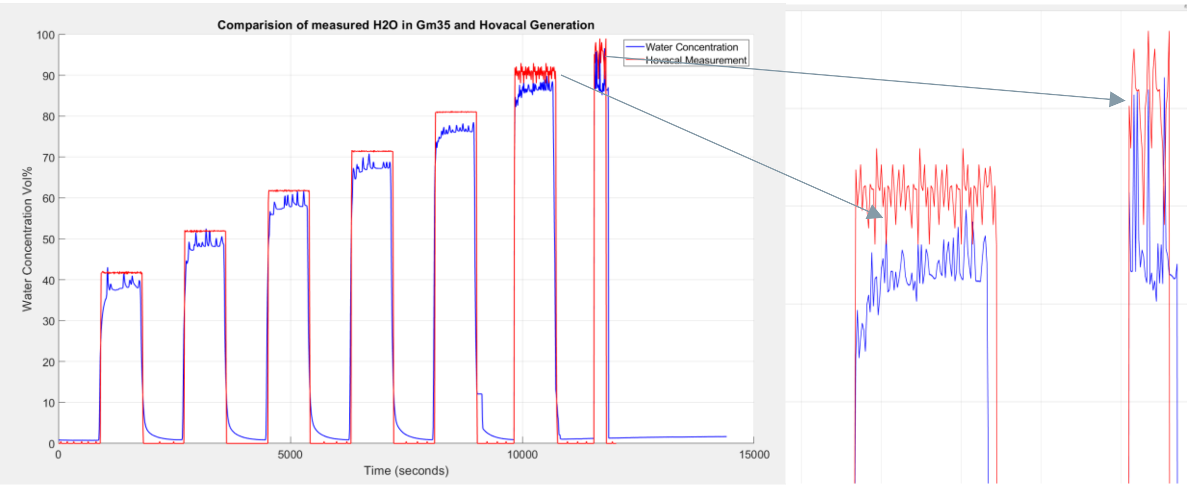

*Figure 9: Comparison of steam generated from HovaCal measured by GM35*

## 6. Task 4.3: Analyser systems for combustion control

In this section the analysers and sensors used for combustion control are shown.

### 6.1. Extractive analysers for combustion control

EHS has designed an extractive gas analysis system to measure $NO_x$ and $CO_2$ concentrations, (and additionally CO, $CH_4$, $H_2O$, $O_2$) which will be used to optimize the combustion process. The system consists of a sampling probe, a sample handling system, and one gas analyser. Both types of analysers are utilized in Tasks 5.3 and 6.2 at the furnace outlet for combustion control measures.

*GM35 - CO, $CO_2$, $H_2O$*

The gas analyser GM35 operates using in-situ optoelectronic technology but for the project it is modified as extractive solution. It calculates the levels of specific gas components by detecting how the gas absorbs light at wavelengths within the measurement path.
In the GM35 gas analyser, light emitted from the sender/receiver unit travels along the measurement path, gets reflected by a mirror at the opposite end, and passes through a beam splitter. This light is then directed through a filter wheel that is adaptable for detecting specific gases like CO, $CO_2$, and $H_2O$. The detector is designed to sense specific wavelengths in the infrared region ranging from 1.6 µm to 4.9 µm, ensuring accurate gas measurements.

*Table 3: Configuration of GM35*

| *Parameters* | |
|---|---|
| *Measurement principle* | *Gas filter correlation, interference filter correlation* |
| *Measured values* | *CO, $CO_2$, $H_2O$* |
| *Type of installation* | *Modified extractive probe version* |
| *Measuring range* | *CO: 0…1,500 ppm*<br>*$CO_2$: 0…24 vol%*<br>*$H_2O$: 0…100 vol%* |
| *Relative error* | *± 2 % full scale value of the measuring range* |
| *Ambient conditions* | *Temperature: +5 °C…+55 °C; absolute humidity ≤ 96 % Relative humidity; non-condensing* |
| *Measuring conditions* | *180 °C (maintained at 180°C to avoid condensation), atmospheric pressure* |

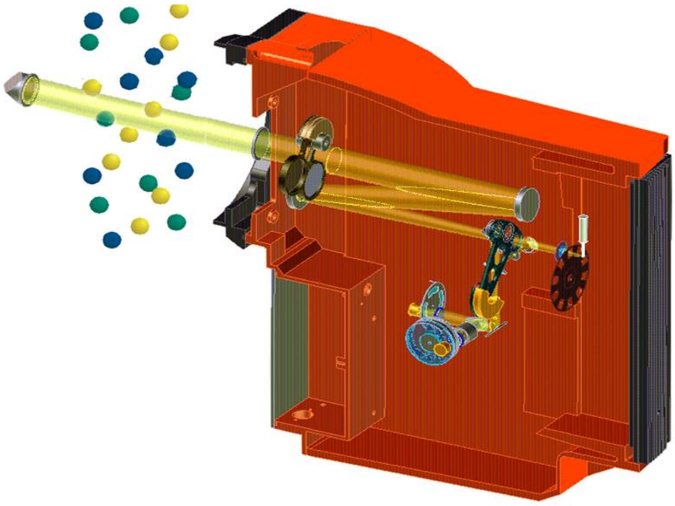

Figure 10: Schematic overview of the optical path of a GM35 analyser [source: Endress+Hauser]

The GM35 gas analyser was tested under controlled laboratory conditions to evaluate its performance across defined measuring ranges. The instrument is configured to detect CO within a range of 0 to 1,500 ppm and $CO_2$ from 0 to 23.5 vol%. During the test, stepwise concentration set points were applied to assess accuracy and response behaviour. Specifically, CO concentrations of 0, 100, 300, and 500 ppm were introduced, along with $CO_2$ levels of 0, 1.0, 1.5, and 2 vol%. This is displayed in Figure 11 and Figure 12.

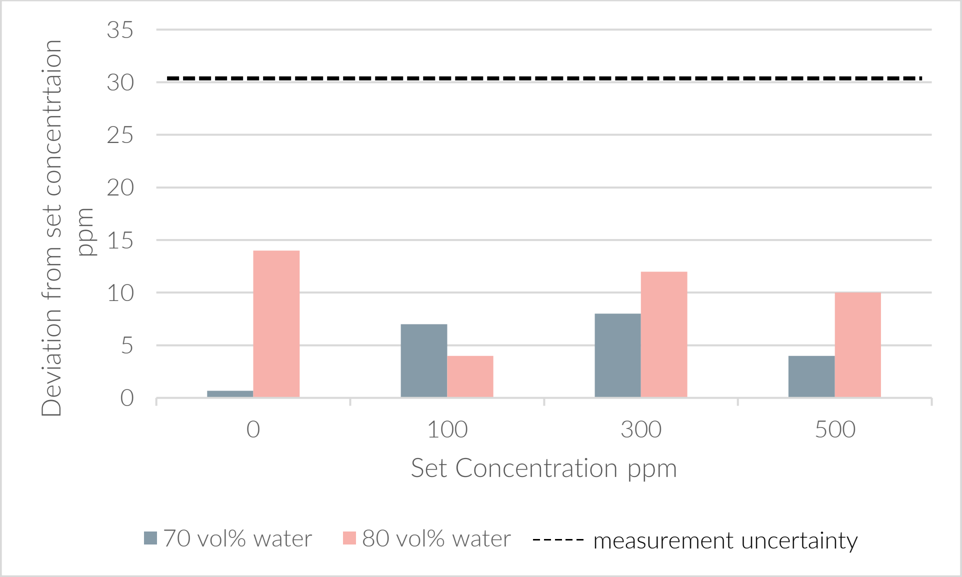

Figure 11: Measured CO concentration in GM35 at high water content

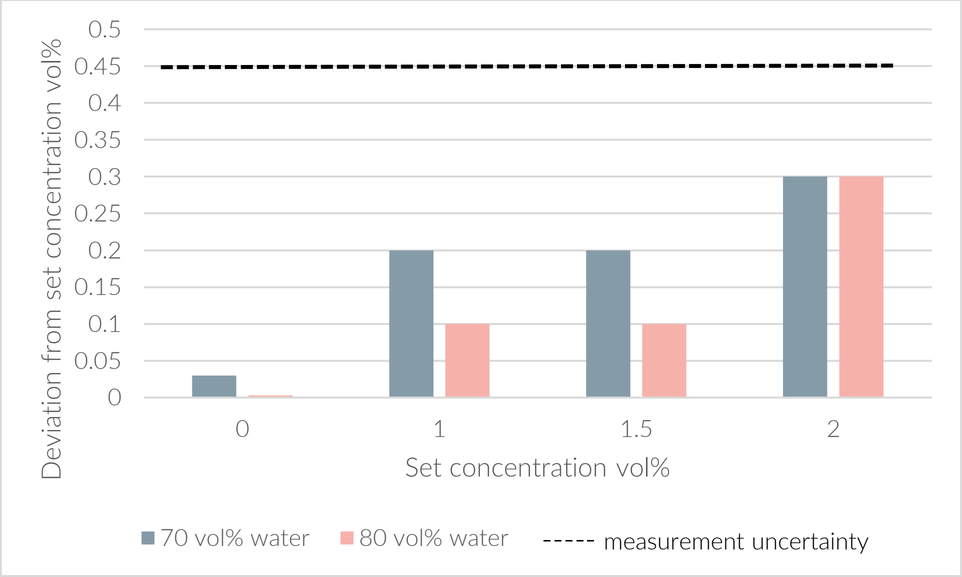

*Figure 12: Measured $CO_2$ concentration in GM35 at high water content*

The influence of water vapour on CO and $CO_2$ measurements was found to be negligible, indicating minimal cross-interference in the GM35 analyser. The relative measurement errors were way below the described error of 2.0%, confirming good accuracy within the tested concentration ranges.

### *MCS300P - $NO_x$, $O_2$, CO, $CO_2$, $H_2O$, $H_2$*

The analyser MCS300P is an extractive process photometer for measuring gaseous or liquid media. It detects IR- and VIS-active components with variable measuring ranges from very low (ppm) to high (vol%) concentrations. It can be adapted towards the application requirements, e.g., optimized sampling system or cuvettes. This analyser is installed at C-TEC facility only and can be seen in Figure 13.

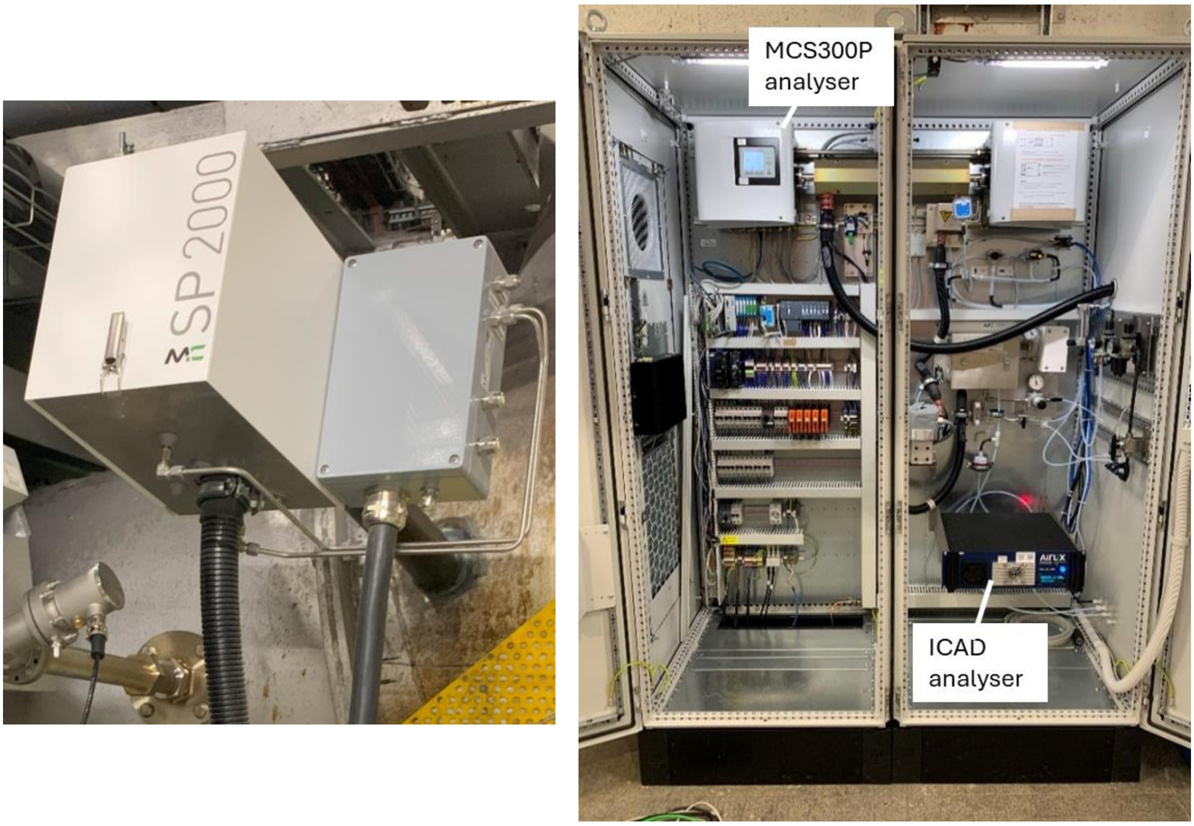

*Figure 13: Installed MCS300P analysing system*
*left: Sample gas probe, right: analysing cabinet with MCS300P and ICAD analyser*

The measurement principle of the included IR photometer is based on the Lambert-Beer Law, which quantifies the absorbance of light as it passes through a sample.
The light's initial intensity ($I_0$) is measured before it enters the sample, and the transmitted intensity ($I_1$) is measured after it passes through. The difference in these intensities, related to the sample's absorbance, helps determine the concentration of the component being measured. To ensure the measurement is within a feasible range for the detector, the path length can be adjusted, especially for low concentrations, as longer path lengths enhance the absorbance signal. Thus, MCS300P adapts by offering different cell lengths to suit various measurement ranges, optimizing accuracy and sensitivity.

*Table 4: Configuration of MCS300P analysing system*

| *Parameters* | |
|---|---|
| *Measurement principle* | *Interference filter correlation, gas filter correlation* |
| *Measured values* | *NO, $NO_2$, CO, $CO_2$, $CH_4$, $H_2O$* |
| *Type of installation* | *Extractive* |
| *Measuring range* | *NO: 0…2,200 ppm*<br>*$NO_2$: 0…1,500 ppm*<br>*$O_2$: 0…21 vol%*<br>*CO: 0…1,500 ppm*<br>*$CH_4$: 0…1,000 ppm*<br>*$CO_2$: 0…30 Vol%*<br>*$H_2O$: 0…100 Vol%* |
| *Accuracy* | ± 1 % full scale value of the measuring range |
| *Ambient conditions* | *Temperature: 5 °C … +40 °C; absolute humidity ≤ 80 % relative humidity; non-condensing* |
| *Measuring conditions* | *185 °C, -0.2…+0.2 bar(g)* |

The MCS300P analyser was tested in the laboratory for the measurement of $H_2O$, CO, NO, and $NO_2$. The measurement range for water vapour extends up to 100 % by volume. On the one hand, the water concentration shall be actively tracked during the combustion. On the other hand, the water measurement is necessary to do the cross-sensitivity correction of the effected measuring components. Due to the high water content, the length of the measurement cell of the analyser was fixed. Therefore, the lowest possible measuring ranges of all other measurement components were set. Consequently, the ranges for NO, $NO_2$ and CO are 2,200 ppm, 1,500 ppm and 1,500 ppm respectively. Although the MCS300P is also capable of measuring $CH_4$, $O_2$, and $CO_2$, these components were not included in the laboratory testing.

During the tests, water vapour concentrations of up to 90 % were evaluated. However, as observed previously with the GM35 in figure 9 the HovaCal system tends to show reduced consistency at steam concentrations exceeding 80%. It is shown in Figure 14.

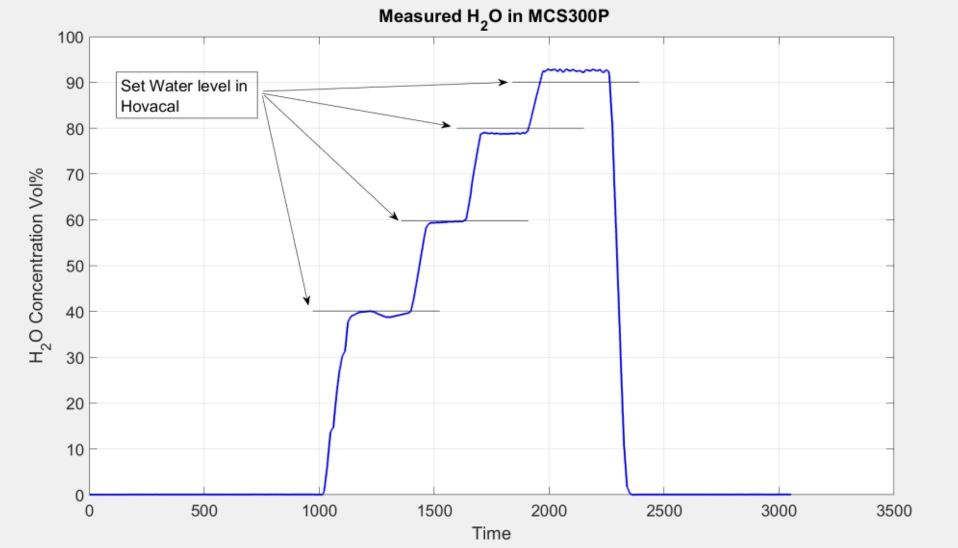

*Figure 14: Measured $H_2O$ concentration by MCS300P*

Due to limitations in the premix gas supply, NO, $NO_2$, and CO measurements were performed at water vapour levels of 60 % and 70 %.

The following set points were tested:

- NO: 125 ppm and 200 ppm
- $NO_2$: 100 ppm and 200 ppm
- CO: 125 ppm and 150 ppm

The measured values were within ±2 % accuracy, demonstrating acceptable performance under high humidity conditions.

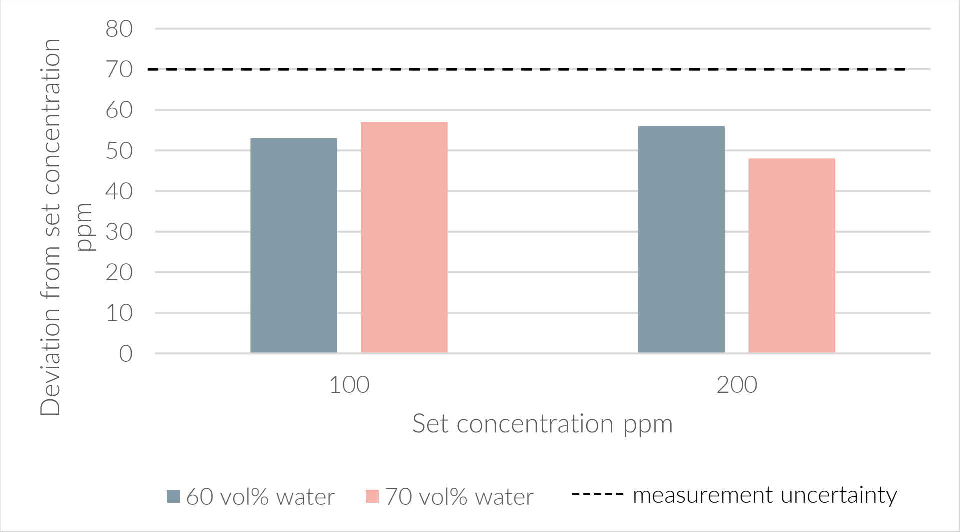

*Figure 15: Measured $NO_2$ by MCS300P at high water content*

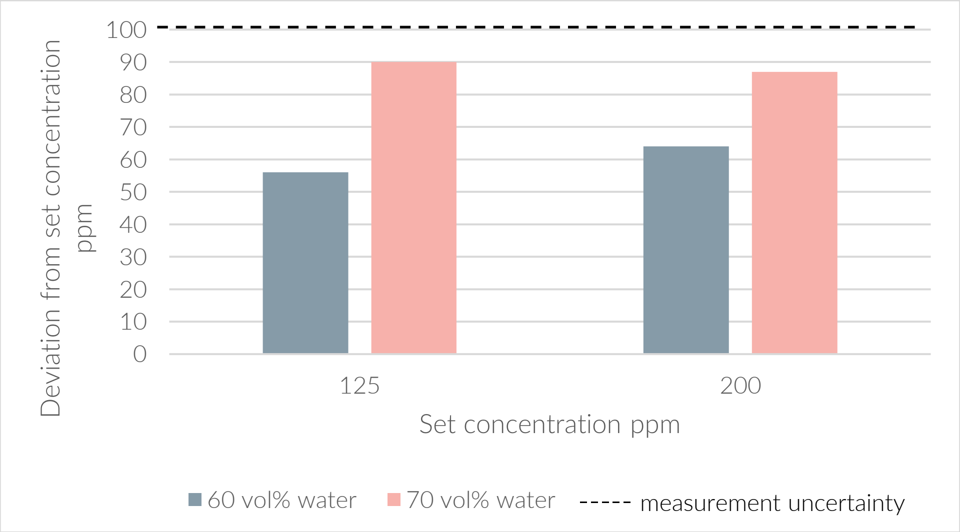

*Figure 16: Measured NO by MCS300P at high water content*

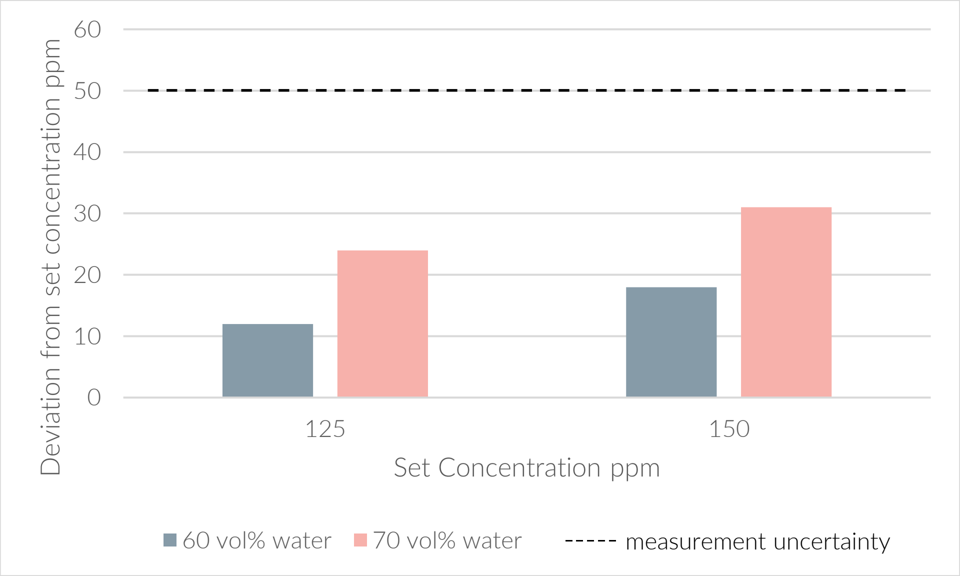

*Figure 17: Measured CO by MCS300P at high water content*

*ICAD $NO_2$/NOx analyser*

Additionally, another $NO_2$/$NO_x$ analyser was added to the extractive analyser cabinet along with MCS300P system as the measurement technique used here has high potential to provide robust and continuous analysis. It is shown in Figure 18.

The technology described is based on ICAD (Intra Cavity Absorption Detection) spectroscopy, which is used for the selective detection of gases like $NO_2$, $NO_x$, etc. This technique involves the use of differential optical absorption spectroscopy (DOAS), where a high-intensity UV light passes through an optical cavity containing the gas sample. The light path within the cavity is greatly extended by reflective mirrors, enhancing the absorption by specific gas molecules. The absorption spectrum, which serves as a “fingerprint" for each gas, is then measured using a spectrometer. The system is highly sensitive and accurate, capable of distinguishing between different gases with minimal interference from other compounds like water vapour or oxygen. This method and the setup in the extractive analysing system also eliminates the need for calibration gases and sample drying, making it particularly effective for continuous emission monitoring in various environments.

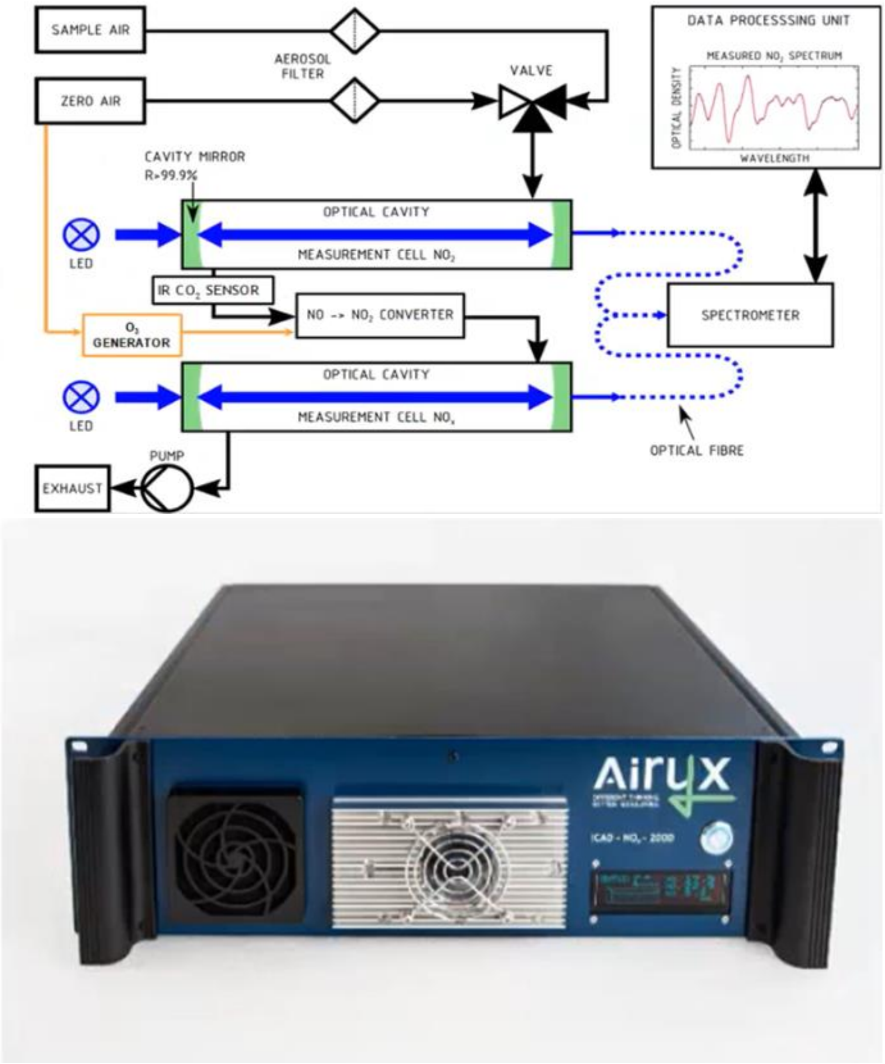

*Figure 18: ICAD $NO_2$/NOx measurement principle and device [source: Airyx]*

*Table 5: Configuration of Airyx ICAD analyser*

| *Parameters* | |
|---|---|
| *Measurement principle* | *UV DOAS* |
| *Measured values* | *NO, $NO_2$* |
| *Type of installation* | *Extractive* |
| *Measuring range* | *NO: 0…10 ppm (Factor of 100 with Dilution Unit)*<br>*$NO_2$: 0…10 ppm (Factor of 100 with Dilution Unit)* |
| *Accuracy* | *± 2 %* |
| *Ambient conditions* | *Temperature: +5 °C…+40 °C* |
| *Measuring conditions* | *40°C at sensor* |

The Airyx ICAD analyser was also tested in the laboratory for the measurement of NO, and $NO_2$. The standard measuring range for both NO and $NO_2$ is 0 to 5 ppm, which was modified to measure 10 ppm and with the use of a dilution unit, this range was extended by a factor of 100, allowing for measurements up to 1000 ppm. The analyser itself was tested at set points of 100 and 200 ppm for both NO and $NO_2$.

The system demonstrates excellent accuracy, with a relative error of ±2 %, as shown in Figure 19 and Figure 20 making it well-suited for applications requiring reliable measurement of nitrogen oxides under varying conditions.

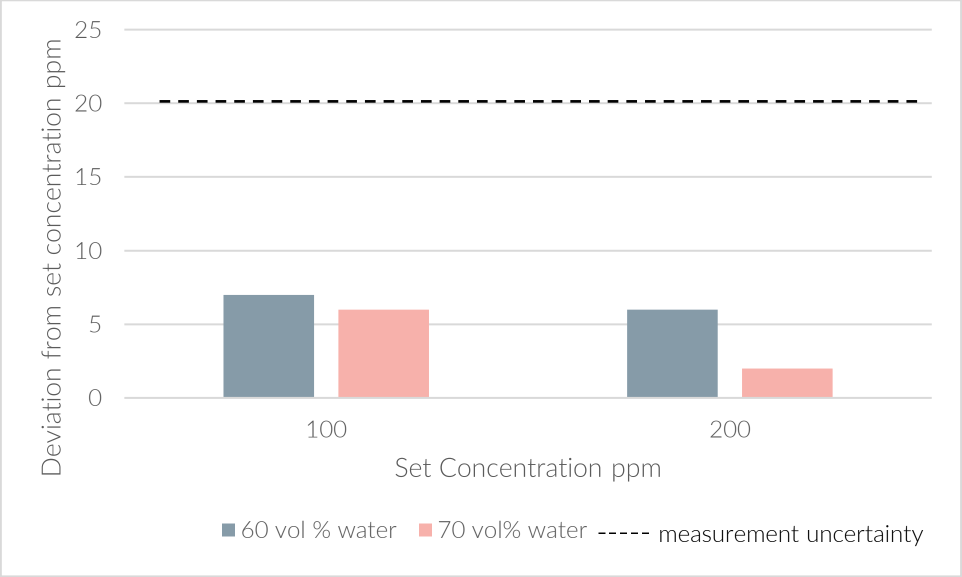

*Figure 19: Measured $NO_2$ by Airyx ICAD at high water content*

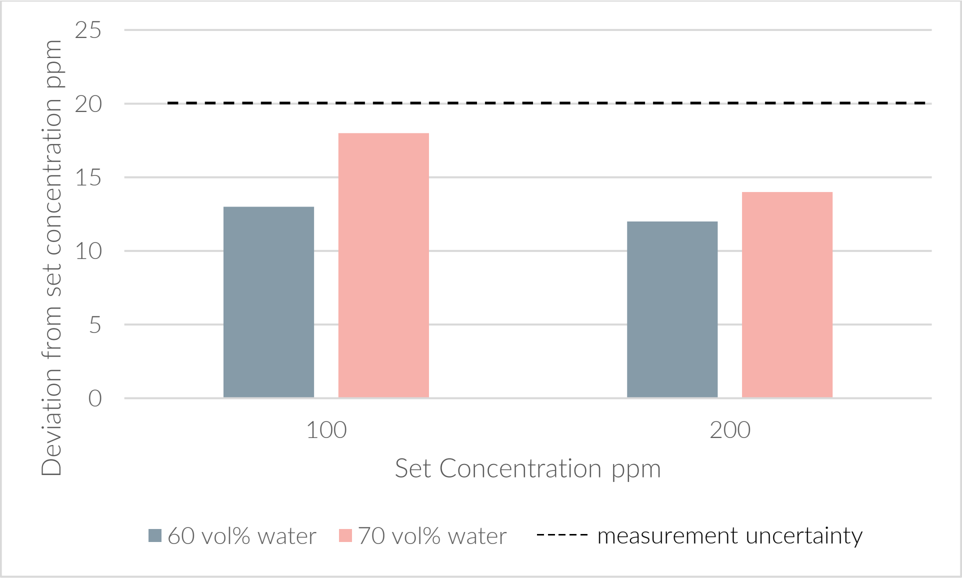

*Figure 20: Measured NO by Airyx ICAD at high water content*

## 6.2. In-situ analysers for combustion control

EHS has collaborated with a supplier of solid-state electrolytic sensors to investigate and, if applicable, improve these sensors for detecting $O_2$, COe and $NO_x$ at high temperatures and high water content. The temperatures of the furnaces at both demonstrator sites are close to 1200 °C. Both types of analysers will be utilized in Tasks 5.3 and 6.2 at the furnace outlet for combustion control measures. Following are the descriptions of the analysers.

*LT3 Transmitter with KS1D probe - $O_2$, COe*

The LAMTEC LT3 Transmitter with KS1D probe for $O_2$/COe measurement utilizes a heated electrochemical cell constructed from zirconium dioxide ceramic ($ZrO_2$). It features three electrodes:

- an $O_2$ electrode made of platinum,
- a $CO_e$ electrode composed of platinum and a noble metal,
- a reference electrode, also made of platinum.

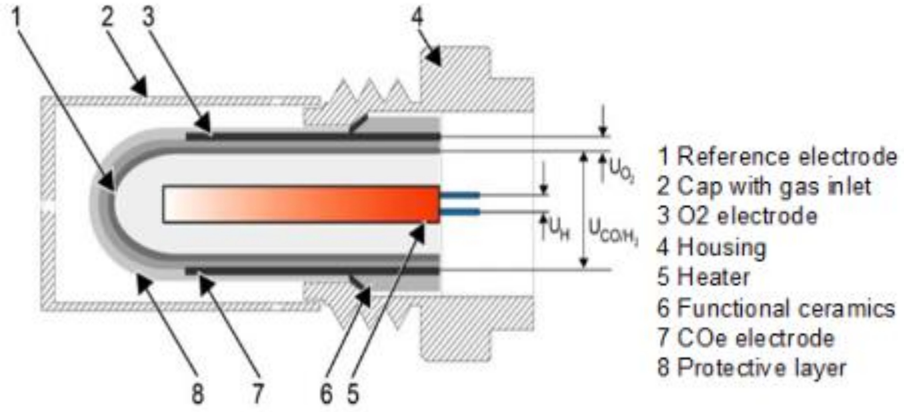

*Figure 21: Design and principle of LAMTEC KS1D sensor [source: Lamtec]*

The probe consists of a zirconium dioxide ceramic tube, sealed at one end. The two measuring electrodes for $O_2$ and COe (CO/$H_2$) are on the ceramic's outer side, within the measuring gas compartment. An integrated heater elevates the probe's temperature to approximately 650 °C and maintains this temperature. At this elevated temperature, the zirconium dioxide ceramic conducts oxygen ions, and the sensor signal voltages $U_{O2}$ between the reference and $O_2$ electrodes and $U_{CO/H2}$ between the reference and COe electrodes are generated and can be measured.

*Table 6: Configuration of LT3 transmitter with KS1D probe*

| *Parameters* | |
|---|---|
| *Measurement principle* | *Zirconium dioxide cell (ZrO2), potentiometric (voltage probe)* |
| *Measured values* | *$O_2$, COe* |
| *Type of installation* | *In-situ* |
| *Measuring range* | *COe: 0…1000 ppm*<br>*$O_2$: 0…10 vol% (0…25 vol%)* |
| Accuracy | $O_2$: ± 5 % of measuring value, not better than ± 0.3 vol%<br>COe: ± 25 % of measuring value, not better than ± 20 ppm |
| *Ambient conditions* | *Temperature: +5 °C…+50 °C* |
| *Measuring conditions* | *350°C at sensor* |

The LT3 was tested for $O_2$ and equivalent COe measurements at high water content. As described above, if any combustible gas is present, it will be measured as COe. In the lab test, hydrogen was supplied which was measured as COe. As described in the Table 6Table 6: Configuration of LT3 transmitter with KS1D probe, the specified measuring range for $O_2$ is 0 to 25 vol%, and for COe, 0 to 1000 ppm. COe concentrations were applied at set points of 100, 200, and 300 ppm and $O_2$ concentrations applied was 2, 3 and 5 Vol% to evaluate the analyser's response and accuracy. The instrument performed consistently within these ranges, supporting its suitability for combustion process monitoring and emissions analysis as shown in Figure 22 and Figure 23.

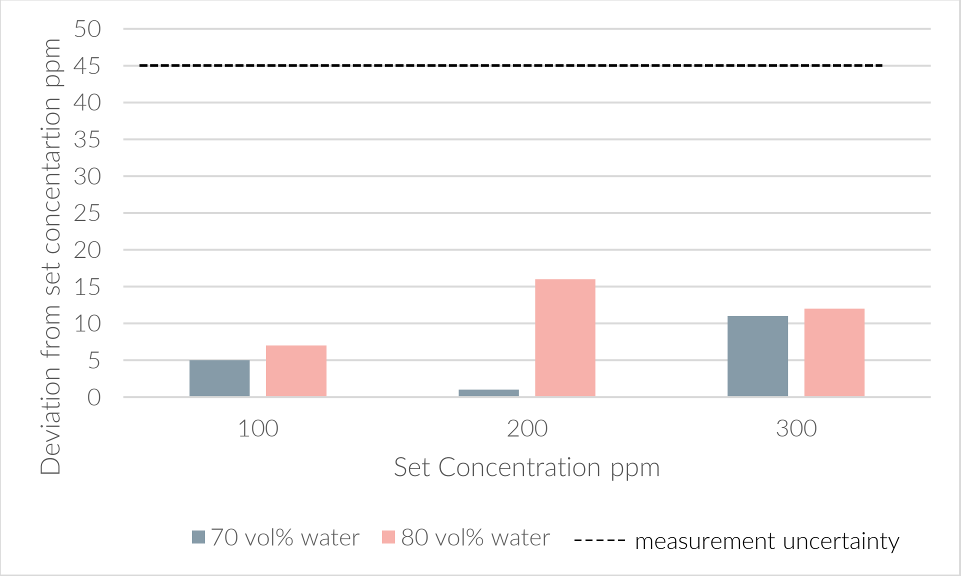

*Figure 22: Measured COe (hydrogen) by LT3 at high water content*

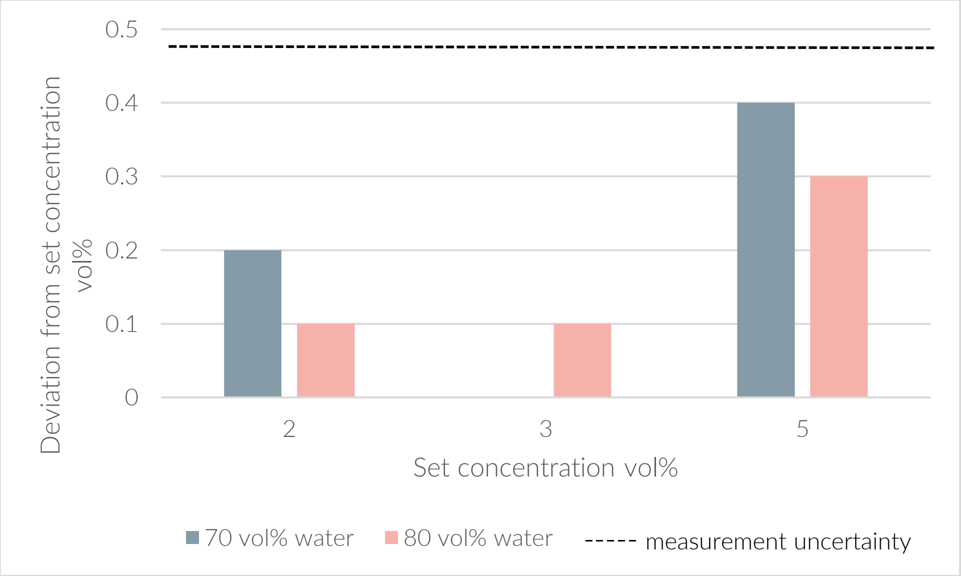

*Figure 23: Measured $O_2$ by LT3 at high water content*

Under ideal laboratory conditions, the analyser showed hardly any deviation even at high water vapour concentrations. The measurement remained stable and unaffected by moisture. The relative error determined during the experiment is below 2 %, which is below the standard accuracy described in the datasheet, confirming the system's robustness and accuracy in humid environments.

### *NT1 Transmitter with KS2DNOx probe - $O_2$, $NO_x$*

Figure 24 shows the principle of the NT1 Transmitter with KS2DNOx probe for $O_2$/$NO_x$ measurement using two electrochemical cells. The first cell measures the initial oxygen concentration, utilizing electrodes connected to a voltage reader. The gas then flows to a second cell, which also measures oxygen concentration. By comparing the oxygen levels before and after the gas passes through the second cell, the system can determine the $NO_x$ concentration based on the difference between the two measurements. This setup allows for accurate monitoring of both $O_2$ and $NO_x$ levels in the gas stream.

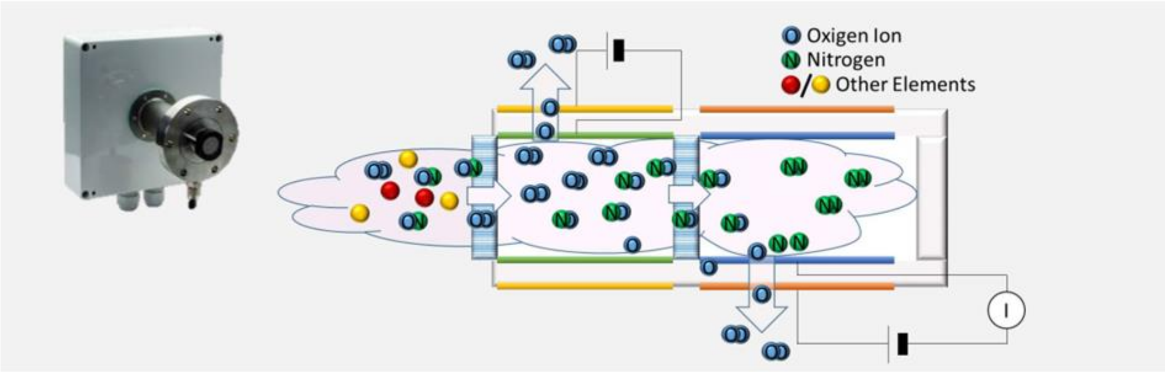

*Figure 24: $O_2$ and NOx measurement principle [source: Lamtec]*

The NT1 analyser has measuring ranges for $O_2$ of 0 to 25 vol% and for $NO_x$ of 0 to 1000 ppm as described in Table 7. $NO_x$ concentrations were applied at set points of 100, 200, and 300 ppm and $O_2$ concentrations applied were 2, 4 and 6 vol% to evaluate the analyser's response and accuracy. The results are shown in Figure 25 and Figure 26. The instrument performed consistently within these ranges, supporting its suitability for combustion process monitoring and emissions analysis.

*Table 7: Configuration of NT1 transmitter with KS2DNOx probe*

| *Parameters* | |
|---|---|
| *Measurement principle* | *Zirconium dioxide cell (ZrO2) combined pumping and Nernstian cell for O2; pumping cell for NOx* |
| *Measured values* | *$O_2$, NOx* |
| *Type of installation* | *In situ* |
| *Measuring range* | *NOx: 0…1,000 ppm*<br>*$O_2$: 0…10 vol% (0…25 vol%)* |
| *Accuracy* | *$O_2$: ± 8 % of measuring value, not better than ± 0.2 vol%*<br>*NOx: ± 10 % of measuring value, not better than ± 3 ppm* |
| *Ambient conditions* | *Temperature: +5 °C…+50 °C;* |
| *Measuring conditions* | *350°C at sensor* |

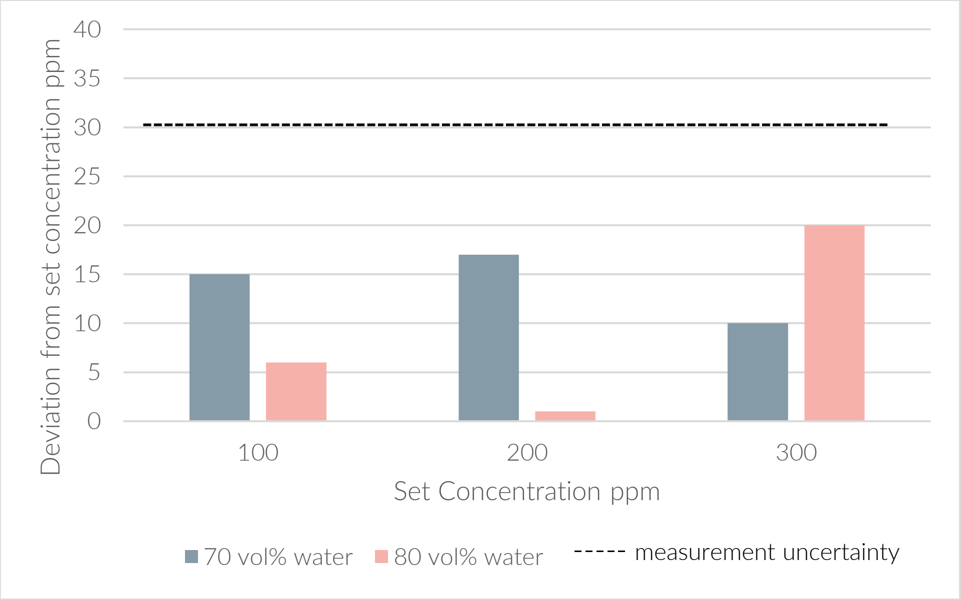

*Figure 25: Measured $NO_x$ by NT1 at high water content*

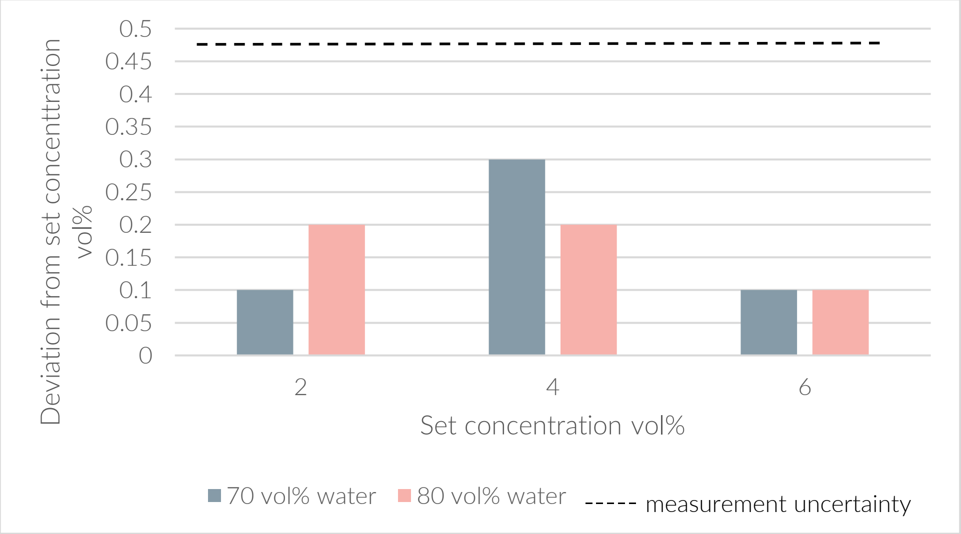

*Figure 26: Measured $O_2$ by NT1 at high water content*

Under ideal laboratory conditions, the analyser showed very little deviation at high water vapour concentrations. The measurement remained stable and unaffected by moisture. The relative error was below 2.5 % which is below the standard accuracy described in the datasheet, confirming the system's robustness and accuracy in humid environments.

# 7. Task 4.4: In situ emission measurement system for $NO_x$, $O_2$ and flow

Measurement requirements and constraints were clarified in WP1. This allows adapting, manufacturing, and testing the relevant sensors for the defined specifications. Three different systems will be used:

- GM32 analyser to measure NO and $NO_2$.
- ZIRKOR200 analyser to measure $O_2$.
- High temperature ultrasonic flow measurement (HT USM) to measure the mass flow.

The development of advanced gas analysers is crucial for optimizing furnace operations by providing precise real-time measurements of gases like $O_2$, $H_2$, $CO_2$, and $NO_x$. These measurements enable efficient combustion control, ensure safety by detecting hazardous gases, and maintain process stability. Apart from that, with emission monitoring it ensures compliance with environmental regulations. By comparing measurements before and after switching from natural gas (C-TEC) and light oil (SWERIM) combustion to cleaner $H_2/O_2$ combustion, guidelines can be established for expected emission levels when implementing cleaner fuels on a larger scale. Precise control of gas compositions improves product quality by monitoring scale formation, descalability, decarbonization, and hydrogen pick-up, and helps understand refractory degradation mechanisms. Additionally, these analysers validate numerical models for process scalability and greenfield designs, driving technological advancements and the adoption of cleaner combustion technologies such as $H_2/O_2$.
Sensor principles and the development status are explained below.

### *GM32 - NO, $NO_2$*

The optimized algorithms of the GM32 evaluation electronics process the measurement signal of the receiving element together with the associated parameters using the DOAS method (Differential Optical Absorption Spectroscopy). The analyser GM32 measures NO and $NO_2$ concentrations by exploiting the unique absorption characteristics of the molecules in the ultraviolet (UV) spectrum. The process involves irradiating the sample gas with UV light, which is absorbed at specific wavelengths by NO and $NO_2$. The analyser then selectively uses these wavelengths to measure the absorption, which directly correlates to the concentration of these gases. Interference filter correlation (IFC) is employed to isolate the specific wavelengths, ensuring accurate measurement by minimizing interference from other gases. This method allows precise determination of NO and $NO_2$ concentrations in the sample gas. Apart from that, UV light does not have any interference to water as it is not active in UV region, ensuring good measurement even in high humid conditions.

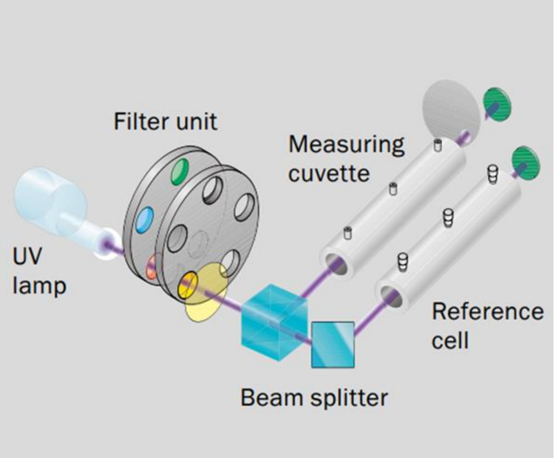

*Figure 27: GM32 measurement principle [source: Endress+Hauser]*

*Table 8: Configuration of GM32*

| *Parameters* | |
|---|---|
| *Measurement principle* | *Differential optical absorption spectroscopy (DOAS)* |
| *Measured values* | *NO, $NO_2$* |
| *Type of installation* | *In situ - cross duct* |
| *Measuring range* | *NO: 0…350 ppm*<br>*$NO_2$: 0…300 ppm*<br>*$SO_2$: 0…200 ppm for cross-sensitivity correction* |
| *Relative error* | *+-2%* |
| *Ambient conditions* | *Temperature: +5 °C…+55 °C; absolute humidity ≤ 96 % relative humidity; non-condensing* |
| *Measuring conditions* | *≤ 700 °C, atmospheric pressure* |

The GM32 analyser was tested for NO and $NO_2$ at high water content as background gas. The specified measuring ranges were 0 to 350 ppm for NO and 0 to 300 ppm for $NO_2$. During the tests, gas concentrations were applied at set points of 0, 50, 100, 150, and 200 ppm for both NO and $NO_2$ as displayed in Figure 28 and Figure 29. The analyser responded reliably across all levels, supporting accurate detection of NOx within typical combustion and emissions monitoring scenarios.

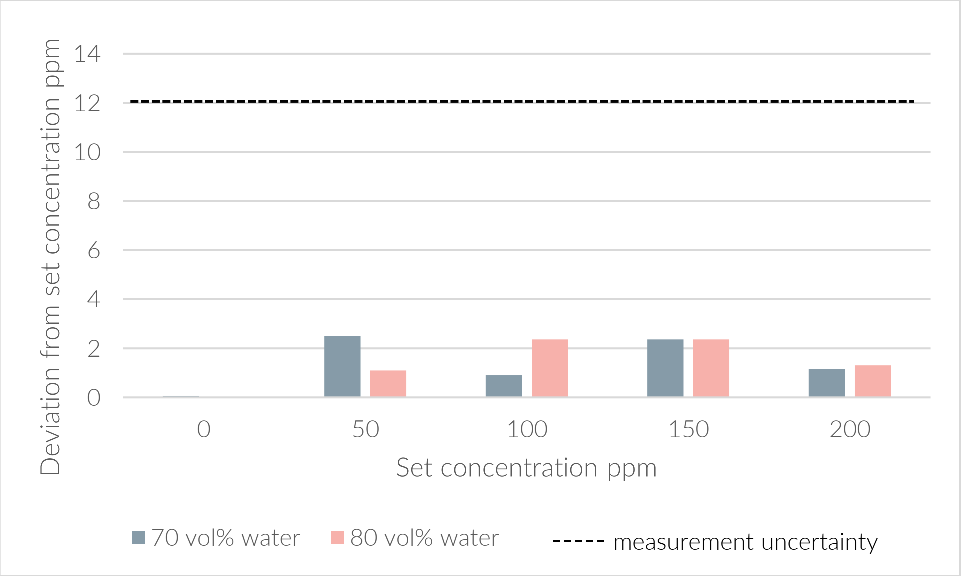

*Figure 28: Measured NO concentration by GM32 at high water content*

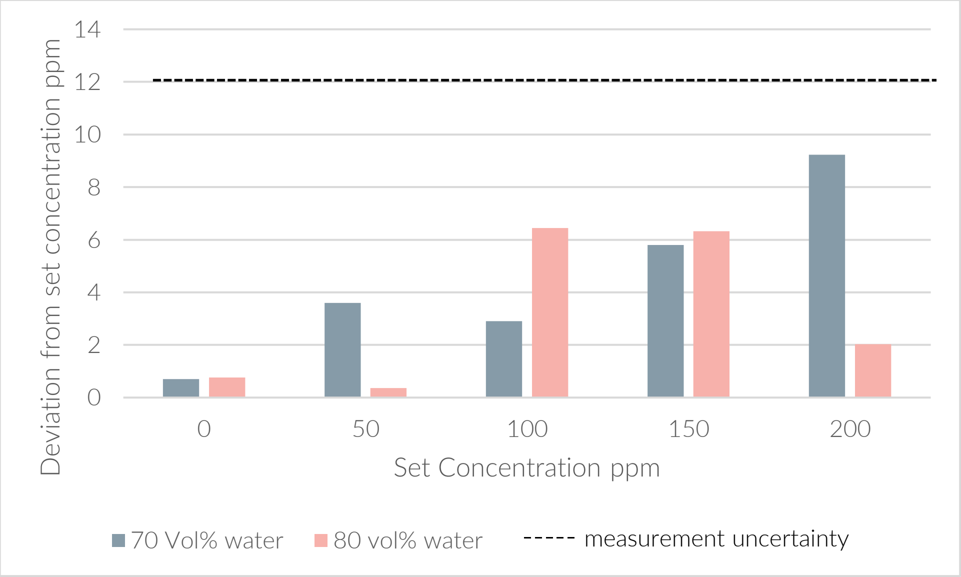

*Figure 29: Measured $NO_2$ concentration in GM32 at high steam*

Under ideal laboratory conditions, even at high water vapour concentrations, the GM32 showed hardly any deviation in the measurement of NO and $NO_2$. The analyser maintained stable and accurate readings, demonstrating strong resistance to cross-interference from moisture. The relative error was way below the described error of 2 % for NO and $NO_2$, confirming the analyser's reliability in humid environments.

*ZIRKOR200 - $O_2$*

A zirconium dioxide sensor measures oxygen concentration by exploiting the electrochemical properties of zirconium dioxide, which becomes an oxygen ion conductor at high temperatures. The measurement gas is led into the zirconium dioxide measuring chamber, where it is heated, causing the oxygen to ionize. Due to the cathodic effect of the $ZrO_2$, a current flows when voltage is applied, providing highly accurate and precise measurements. The sensor consists of a zirconium dioxide ceramic tube with platinum electrodes and a heater to maintain high temperature. The generated voltage, determined by the Nernst equation, is proportional to the logarithm of the oxygen partial pressure ratio between the reference (ambient air) and the measured gas. Calibration can be performed with ambient air, making the measurement process highly accurate and efficient without the need for test gases.
ZIRKOR200 was not tested in the lab as it uses a zirconium dioxide sensor which is a state-of-the-art measurement for oxygen in industrial setup.

*Table 9: Configuration of ZIRKOR200*

| *Parameters* | |
|---|---|
| *Measurement principle* | *Zirconium dioxide cell (ZrO2)* |
| *Measured values* | *$O_2$* |
| *Type of installation* | *In-situ* |
| *Measuring range* | *$O_2$: 0…25 vol%* |
| *Accuracy* | *±0.5 % of measuring value or ± 0.02 vol%* |
| *Ambient conditions* | *Temperature: +5 °C…+40 °C* |
| *Measuring conditions* | *700 °C at sensor* |

*High temperature ultrasonic measurement - flow, temperature*

The measurement of the exhaust mass flow in the chimneys of the demonstrators is a new challenge due to higher temperatures. The adaptation and optimization of the ultrasonic flow measurement for high temperatures requires significant development capacities. The standard ultrasonic transducers developed by EHS have temperature resistance till 280 °C. For this project an extended temperature range between 350 °C up to 400 °C is needed. Therefore, one main focus is on optimizing the materials and joining technologies in order to achieve high-temperature stability. Secondly a measuring device (transducer, electronics, temperature sensor, etc.) is adapted to the SWERIM demonstrator needs. Figure 30 shows a 3D model of the high temperature flow measurement prototype (3), the temperature measurement (2), the signal processing unit (1) and how it is installed at SWERIM exhaust chimney. The chimney is isolated with a second outer pipe which is not shown in the 3D model.

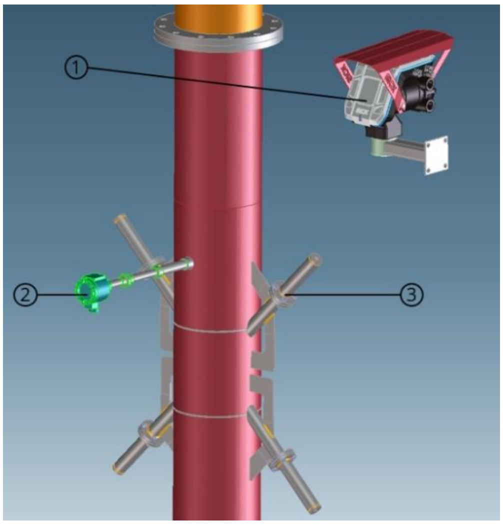

*Figure 30: 3D model of high temperature ultrasonic flow meter in the SWERIM demonstrator [source: Endress+Hauser]*

Figure 31 shows the installation of the flow meter at SWERIM. Due to unexpected higher temperatures during initial tests with new burners at SWERIM, the sensors were exposed to excessively high gas temperatures (above 600 °C), which led to irreversible damage of the ultrasonic sensors. Measurement data are not available. It is planned to install new sensors in August 2025.

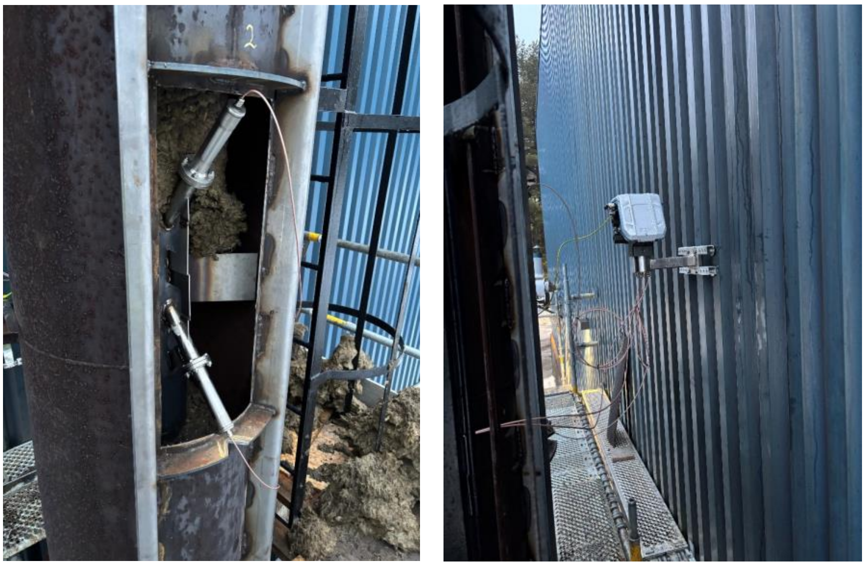

*Figure 31: HT pilot flow meter installation at SWERIM*
*Left: ultrasonic transducer installation; right: signal processing unit*

# 8. Task 4.5: Concept for predictive emission monitoring (PEM)

Predictive emission monitoring systems (PEMS) are an approach for the continuous monitoring of emissions as a supplement to the continuous measurement and documentation of the measuring emission values. For this purpose, an empirical model is developed which establishes the relationship between characteristic and easily accessible process and environmental data, e.g., gas temperature or oxygen content, and the corresponding emission measuring values.
PEMS can thus support continuous real-time monitoring of pollutants such as nitrogen oxides, $SO_2$, CO and ensure uninterrupted documentation.

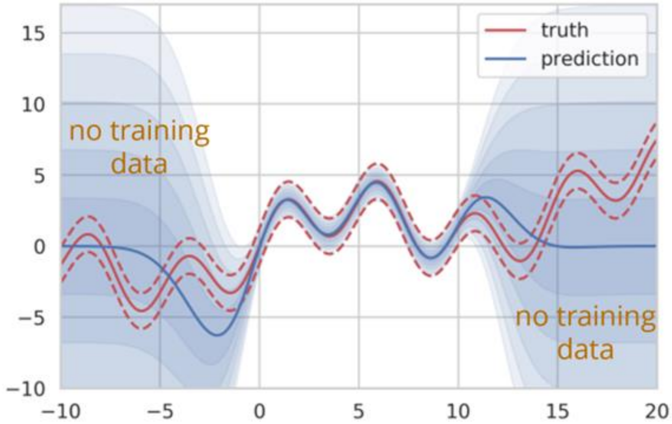

*Figure 32: Visualization and comparison of measured and predicted measuring values [source: Endress+Hauser]*

Within this work package, PEMS concepts were developed for the two furnaces of the demonstrator test facilities at C-TEC and SWERIM. It includes the planned procedure to build up the calculation model and the data storage and infrastructure included in the system cabinets. Initial models can be created after measuring values in the different operation modes, e.g., different oxygen contents, hydrogen-natural gas ratios or combustion temperatures and other process conditions are available.
Once the initial model has been created, it will be trained using the necessary values from the installed continuous emission monitoring systems (CEMS). For better adaptation towards the real measuring values, different operating modes of the furnace shall also be implemented in the model.

## 9. References

[1] W. Dudley, Methods of experimental physics ; v13, Manhattan, Kansas: Academic Press, 1976

[2] J. Hearnshaw, Astronomical spectrographs and their history, Cambridge, 2009.

[3] H. Pauna, M. Aula, S. Kaukonen, M. Huttula and T. Fabritius, "Optical Emission Spectroscopy as a Tool for Process Control of Steelmaking Burner," in *8th International Congress on the Science and Technology of Steelmaking*, Montreal, Canada, 2022.

[4] M. Aula, A. Leppänen, J. Roininen, E.-P. Heikkinen, K. Vallo, T. Fabritius and M. Huttula, "Characterization of Process Conditions in Industrial Stainless Steelmaking Electric Arc Furnace Using Optical Emission Spectrum Measurements," *Metall. Mater. Trans. B*, vol. 45, pp. 839-849, 31 1 2014.

[5] H. Pauna, M. Aula, J. Seehausen, J.-S. Klung, M. Huttula and T. Fabritius, "Industrial Ladle Furnace Slag Composition Analysis with Optical Emissions from the Arc," *ISIJ Int.*, vol. 60, no. 9, pp. 1985-1992, 2020.

[6] A. Rautioaho, H. Pauna, M. Jokinen, O. Seppälä, E. Busson, L. Sankowski, V.-V. Visuri and T. Fabritius, "Applicability of Optical Emission Spectroscopy for Industrial Flame Analysis with Hydrogen and Natural Gas Mixtures Based on Laboratory Study," *Applications in Energy and Combustion Science,* vol. 22, p. 100329, 2025.

[7] F. Goulay, P. Schrader and H. Michelsen, "Effect of the wavelength dependence of the emissivity on inferred soot temperatures measured by spectrally resolved laser-induced incandescence," *Appl. Phys. B: Lasers Opt*, vol. 100, pp. 655-663, 2010.

# Get in touch

Website

http://hyinheat.eu/

Email address

info@hyinheat.eu